NASA Technical Memorandum 101733

Single-Strain-Gage Force/Stiffness Buckling Prediction Techniques On A Hat-Stiffened Panel

Larry D. Hudson and Randolph C. Thompson

February 1991

National Aeronautics and
Space Administration

NASA Technical Memorandum 101733

Single-Strain-Gage Force/Stiffness Buckling Prediction Techniques On A Hat-Stiffened Panel

Larry D. Hudson
NASA Ames Research Center, Dryden Flight Research Facility, Edwards, California

Randolph C. Thompson
PRC Systems Services, Edwards, California

1991

NASA

National Aeronautics and
Space Administration
Ames Research Center
Dryden Flight Research Facility
Edwards, California 93523-0273

SINGLE-STRAIN-GAGE FORCE/STIFFNESS BUCKLING PREDICTION TECHNIQUES ON A HAT-STIFFENED PANEL

Larry D. Hudson
NASA Ames Research Center
Dryden Flight Research Facility
Edwards, California

Randolph C. Thompson
PRC Systems Services
Edwards, California

ABSTRACT

Predicting the buckling characteristics of a test panel is necessary to ensure panel integrity during a test program. A single-strain-gage buckling prediction method was developed on a hat-stiffened, monolithic titanium buckling panel. The method is an adaptation of the original force/stiffness method which requires back-to-back gages. The single-gage method was developed because the test panel did not have back-to-back gages. The method was used to predict buckling loads and temperatures under various heating and loading conditions. The results correlated well with a finite element buckling analysis. The single-gage force/stiffness method was a valid real-time and post-test buckling prediction technique.

NOMENCLATURE

D	bending strain, μin./in.
DACS	data acquisition and control system
e	distance, in.
F	applied compression load, lb
F/S	force/stiffness method
ΔT	temperature change from ambient, °F

INTRODUCTION

Advances in hypersonic vehicle technology have lead to the development and fabrication of new potential fuselage and wing panel designs. One design that has been fabricated by the McDonnell Douglas Corporation (St. Louis, Missouri) is a hat-stiffened panel. This panel is designed to carry loads both parallel and perpendicular to the hat stiffeners. Their buckling characteristics are critical to the design of these panels. Determining these characterisitics under a variety of thermal-mechanical loads while ensuring panel integrity has required modifications and extensions to an existing experimental technique.

The National Aeronautics and Space Administration (NASA) Ames Research Center, Dryden Flight Research Facility (Ames-Dryden), in a cooperative effort with the McDonnell Douglas Corporation, has completed a test program in which a hat-stiffened panel was nondestructively tested to define its buckling characteristics. The buckling characteristics presented in this paper are limited to general instability load and temperature predictions based on the average of multiple strain gage measurements.

The buckling characteristics of hypersonic vehicle test panels have been evaluated in the past and the experimental techniques have produced good correlation with analysis (Jones and Greene, 1974). From the extensive work that has been accomplished in developing new experimental techniques to help understand panel buckling, the force/stiffness (F/S) method has proven to be a good predictor of local and general instability loads for nondestructive testing (Jones and Greene, 1974). Ko et al. (1986) used this method extensively in defining the buckling characteristics of hypersonic aircraft wing tubular panels under combined heating and loading test conditions. Ko et al. (1986) reported that the test data correlated fairly well with the theoretically predicted buckling interaction curves.

The panels investigated by Ko et al. were symmetric about a neutral plane running the length of the panel. This symmetry allowed back-to-back strain

gages to be used. This paper discusses a panel which is asymmetric about a neutral plane running the length of the panel. The panel has individual hat stiffeners spotwelded to a flat skin. A load frame is also bolted to the panel on all four edges. Therefore back-to-back gages about the neutral plane could not be used. Back-to-back gages are needed to use the F/S method of Jones and Greene (1974), but by modifying the method a single gage can be used to characterize buckling behavior. Consequently, a single-strain-gage F/S method has been developed using the principles of the original method.

This paper discusses the development and application of the single-gage F/S method and its use in testing a hat-stiffened panel. This paper also shows variations of this method used to predict buckling loads under transient heating and to predict a buckling ΔT (elevated temperature – room temperature).

The results shown cover typical experimental data and will not cover every test configuration. The test predictions will be compared with the results obtained from the McDonnell Douglas NASTRAN buckling analysis.

TEST ARTICLE AND SETUP DESCRIPTION

The article that was studied and that the single-gage force/stiffness method was developed on is a hat-stiffened, monolithic Ti 6Al-4V buckling panel. It is representative of a fuselage or wing skin panel for a future hypersonic vehicle (fig. 1). The panel measures 2 ft^2 and 1 1/4 in. thick (including height of hat stiffeners) and has 8 hat stiffeners attached by 64 spot-welds (32 for each stiffener flange) to a flat skin. Both the skin and the hats are 0.032 in. thick. L-shaped and T-shaped frames are bolted to all four sides of the panel to produce a load frame, as shown in figure 1. The panel is designed to carry loads both parallel (axially) and perpendicular (cross-corrugation) to the hat stiffeners and is therefore buckling critical in both the axial and cross-corrugation directions.

To obtain accurate and complete measurements for validating buckling prediction codes, the panel was instrumented with 280 sensors. The instrumentation included 112 Micro-Measurement (Raleigh, North Carolina) foil strain gages (WK-06-062-AP), 156 Type K (Chromel-Alumel, Hoskins Manufacturing Co., Hamburg, Michigan) thermocouples, and 12 deflection potentiometers. Figure 2(a) shows instrumentation on the skin side of the panel. Strain gages were positioned in both the axial and cross-corrugation directions and were distributed over the panel to provide an overall understanding of the panel behavior. The deflection potentiometers were evenly distributed throughout the panel to measure out-of-plane deformations and were attached to the skin side of the panel between the legs of each hat stiffener. Figure 2(b) shows the hat-stiffened side of the panel. Strain gages were positioned in line with the hats and were located on the cap and legs of the hat stiffeners. Thermocouples were distributed on both sides of the panel and on the loading frames to record panel temperature distributions.

Compressive loads were applied to the panel in the 220-kip uniaxial load frame system shown in figure 3. The load frame system primarily consists of an upper and lower load platen, a moveable hydraulic ram, a load cell, and a chain-mail screen. The load cell has a precision of 0.1 percent of reading and the data acquisition system has a precison of ± 1 count or approximately ± 50 lb. Therefore a 50,000-lb load is precise to ± 100 lb.

A major emphasis of the test setup was producing an adequate and definable thermal environment surrounding the panel to correlate both temperature and strain measurements with analysis. The three controllable boundary conditions that were taken into account during the initial test apparatus design were the load platens, insulated water-cooled side frames, and quartz lamp oven. Figure 4 shows details of the platen design. The load platens consist of a heated platen with embedded electrical resistance heaters and a water-cooled platen separated by a piece of 1/4-in. semirigid insulation. The heated platen maintained a uniform temperature distribution along the edges of the panel perpendicular to the load. The water-cooled platen protected the load cell and load frame system from the elevated temperatures. These platens also ensured better temperature distributions and thermal control.

The insulated, water-cooled side frames were used in specific tests to keep the edges of the panel (perpendicular to the load) near room temperature. In these tests room-temperature water was run through copper tubing brazed along the length of the frame. These frames were also well protected from the radiant lamps by ceramic insulation and highly reflective metallic foil (fig. 5(b)).

The quartz lamp oven shown in figure 5 is an aluminum sheet box lined with ceramic block insulation which was lowered around the panel. Forty-eight 36 in. long quartz lamps backed with ceramic reflectors were positioned horizontally on both sides of the panel, as shown in figure 5(b). The 48 quartz lamps were divided into 8 closed-loop temperature control zones, 4 on each side. Ceramic fences (not shown) were placed between each of the control zones to minimize the natural convection effects and to ensure good thermal control. The lamps were designed to extend beyond the edge of the panel to minimize end effects.

Data acquisition, signal conditioning, and direct digital thermal control were accomplished using the Ames-Dryden Thermostructures Research Facility's data acquisition and control system (DACS) (Zamanzadeh et al., 1987). The primary function of the DACS is to conduct real-time thermal and mechanical simulation of flight environments on test articles and aircraft. The system can record 1280 channels of data of which there can be up to 512 thermal and up to 64 mechanical control channels. DACS also provides real-time visual data analysis displays such as x-y plots, thermal control deviation displays, alphanumeric displays, and F/S displays. The DACS maximum allowable system measurement error is ± 0.15 percent of reading or $\pm 20\ \mu$V, whichever is greater. Therefore, for a $\pm 20\ \mu$V strain measurement input from a single active arm strain gage with a 4 V direct current (DC) excitation voltage, the error band is $\pm 8\ \mu$in./in. This error is reduced with additional active arms and higher excitation voltages. Similarly, a Type K thermocouple measurement error with a $\pm 20\ \mu$V input is equivalent to ± 0.9 °F.

FORCE/STIFFNESS TECHNIQUE AND TEST METHODS

The F/S technique was developed by Jones and Greene (1974) to predict buckling loads in nondestructive tests. The method uses a simple plotting procedure to predict local and general instability loads. The name of the method is derived from the plotting variables: load (force), and load divided by strain (stiffness).

Figure 6 shows a typical F/S plot of the classical buckling case. The load axis (denoted by F) represents compression, shear, or combined loading. The stiffness axis is denoted by F/D where D represents displacement, strain (such as bending), or generalized strain. When local buckling is the critical mode, the value of D should be the generalized strain variable (equation (10) in Jones and Greene, 1974). In using the generalized strain variable, the critical strain components of compression, bending, and shear must be known. The components are obtained from analytical solutions adjusted with empirical data. These empirical data or "knockdown" factors are obtained from destructive testing of subscale test articles (Greene, 1974). The generalized strain variable will not be considered here because overall panel buckling is considered the critical mode for the hat-stiffened panel. In addition, no subscale specimens for destructive testing or analytical solutions were available at the time of testing. In this situation, D represents the bending strain.

The bending strain is usually determined from the difference between back-to-back gages installed parallel to the applied load. The back-to-back configuration cancels out the axial strain component. Instrumenting gages back-to-back was impractical on this panel. Instrumentation would have needed to occur before fabrication and the instrumentation was not expected to survive the fabrication process. Therefore, an attempt was made to simulate back-to-back gages by using the available instrumentation layout on the panel.

Figure 7 shows the typical layout of the instrumentation on the panel. The eccentric gage configuration (fig. 7(a)) uses two gages, one located on the skin side and the other on the cap of the hat stiffener. These gages are not equidistant from the neutral axis of the panel, therefore their difference does not provide a true measure of the bending strain. The offset gage configuration (fig. 7(b)) uses two gages located on the same side of the panel separated by distance e. In this case, one of the gages (gage 2 or 3) responded almost linearly with load throughout a test. This gage is used to represent the response of the gage positioned where bending is being determined (gage 1) if it had responded linearly with load throughout the test. The slopes of the linear portions of gages 1 and 2 or 1 and 3 must be close so an accurate bending strain (at gage 1) can be determined from the difference between the two outputs. This approach may not be practical, because of the difficulties in finding a gage that has a linear response throughout a test or finding gages with similar linear slopes. Local load path variations can also make correlating the outputs of the two gages difficult. To bypass these difficulties and uncertainties in the two

gage approach, a method was developed to determine the local bending strain using a single gage.

The single-gage method divides the gage output into two parts, the linear response and the nonlinear response. Figure 8(a) shows the typical response of a gage to load under uniaxial compression in a buckling situation. Notice the two distinctly different parts to the curve. The gage responds linearly up to a given load, after which bending is introduced and it responds nonlinearly. The single-gage method uses the linear response of the gage to determine the bending strain during the nonlinear response portion. By fitting a straight line through the linear portion, one can linearly extrapolate beyond the bending introduction point. The assumption is that if the gage had continued to respond linearly with load, the output of the gage would have followed the dashed line. The extrapolation beyond the bending introduction point enables one to compute the bending strain at a given load as the difference between the indicated strain and the strain from the linear extrapolation. The bending strain can then be used in the F/S plot.

Figure 8(b) is a typical F/S plot where the variable D is the bending strain. By plotting F/D as a function of F, the characteristic curve results. As the critical buckling load is approached, the curve moves downward to the right. By selecting a linear-fitted range, a line can be extrapolated down to the load axis and thereby predict the buckling failure load. This is the load at which D or the bending strain goes to infinity and F/D approaches zero. This prediction is based on the assumption that no load path or mode changes will occur before the intersection. All of the predictions are of the first mode elastic buckling load, which is considered the critical buckling load. The case is for a typical room or elevated temperature condition.

A variation of the single-gage method has also been used to predict a ΔT which would produce buckling for elevated temperature cases with a known ΔT across the panel. The ΔT is created by maintaining the frames, which are parallel to the load and perpendicular to the platens, at room temperature while heating the panel to an elevated temperature. This produces a hot-panel-to-cooled-frame temperature gradient, introducing a compressive thermal load into the panel.

Figure 9(a) shows an expected strain gage response to temperature. The panel was heated to predetermined uniform temperatures then allowed to reach equilibrium (the state at which transient strains are relieved) at each temperature. The strain value was then noted. During the lower temperatures (T_o, T_1, and T_2), the gage responds linearly once equilibrium has been attained. At temperature T_2, the onset of buckling is reached and the gage goes nonlinear, which is the result of the ΔT across the panel. The linear portion is fitted with a straight line and extrapolated to the higher temperatures. A projected bending curve is drawn by fairing a curve through the symbols from T_2 to T_6. This curve represents what the output of the strain gage would have been if a state of thermal equilibrium had been maintained throughout the temperature profile. The difference between the projected bending curve and the extrapolated line is a measure of the bending in the panel caused by the ΔT. These values are then used in what may be termed a temperature/stiffness plot, as shown in figure 9(b). A buckling ΔT can be determined by the linear extrapolation through the lower $\Delta T/D$s.

The single-gage method has also been adapted to predict buckling loads for constant load transient heating tests. Figure 10(a) shows a typical strain gage response to load and transient heating. A through-the-thickness temperature gradient is obtained on the panel by heating only the skin side while allowing the hat side to rise in temperature. The linear portion of the curve is the part leading to a predetermined load (L_1) with no heating. After the test load is attained, the transient heating begins and the gage starts to respond to structural changes caused by temperature gradients (apparent strain has been accounted for). The gage output is monitored to note the maximum strain attained during the transient heating cycle. This value is assumed to be the maximum bending strain achieved, for that gage, during the test and is assumed to be caused by one-side heating, which induces bowing in the panel. The procedure is repeated for higher constant loads (L_2 and L_3) and the F/S plot of figure 10(b) is obtained. By linearly extrapolating through the F/D values, a prediction of the buckling load under a given transient heating condition can be determined. The value and meaning of this prediction is subject to the type or degree of support the panel has on the edges parallel to the load. Because these boundary conditions are not completely understood for this test, the last application of the single-gage F/S method is given as a potential use of the method.

TEST PROCEDURES

During thermal-mechanical testing, the titanium buckling panel was subjected to a series of nondestructive tests in multiple panel configurations. The panel was first mechanically loaded at room and elevated temperatures with and without the water-cooled frames. The panel was also held at constant loads ranging from 2500 to 3000 lb while an elevated temperature profile was applied. Finally, the panel was held to a constant preload of 500 lb while a through-the-thickness temperature gradient was applied. An extensive test matrix was followed to provide test data for a variety of thermal-mechanical test configurations. The different thermal-mechanical test configurations are shown in figure 11.

To achieve the test configurations shown in figure 11, the panel boundary conditions had to be well defined and stable. The relatively large mass of the load platens created heat sinks that could significantly affect the panel boundary conditions and the thermal closed-loop control. This problem was alleviated by a combination of heated and actively cooled platens. A heated platen with embedded electrical resistance heaters was placed next to the panel while the loading platen was protected from thermal effects by a water-cooled platen. A piece of 1/4-in. semirigid insulation was placed between the heated and cooled platens to protect the load frame from the heat, to prevent heat loss to the cooled platen, and to prevent warping of the loading platens. This design allowed ambient temperatures to be maintained on the upper and lower loading platens and ensured proper load alignment while providing a uniform temperature at the panel ends. The heated platens were manually controlled and not part of the automated thermal control system. The procedure for an elevated temperature test was to heat the heated platens first, because of the platen mass and inherent thermal inertia. When the temperature of the heated platens reached 30–40 °F above the panel temperature, the closed-loop temperature control on the panel was started.

Load alignment and distribution were considered critical to prevent eccentric loading, prevent premature panel buckling, and create uniform load distributions. Load alignment and distribution was ensured by securing the panel in guides attached to the platens, shimming the top and bottom edges of the panel with thin gage foil, and checking the strain gage outputs near the top, bottom, and center of the panel.

To ensure panel integrity, a real-time two-gage and quasi-real-time single-gage F/S evaluation was conducted. Software was developed on the DACS for a real-time display of the F/S method, where an attempt was made to use the two gage approach shown in figure 7. For the single-gage method, a hand-held calculator was used to calculate F/S parameters, and a personal computer was used to plot the F/S method and determine buckling loads. The single-gage method has recently been made available on the DACS. The single-gage method was eventually used as the method of choice, because it determined panel integrity more accurately.

RESULTS AND DISCUSSION

The buckling prediction techniques were divided into three cases: room and elevated temperature buckling load prediction, transient temperature buckling load prediction, and buckling ΔT prediction. The results for each case will be for the single-gage F/S approach.

For the room and elevated temperature buckling load prediction case, the panel was loaded both at room temperature and at an elevated temperature equilibrium condition (figs. 11(b) and (c)). The panel was loaded incrementally to allow for real-time assessments of the F/S method buckling predictions. Figure 12(a) is a typical plot of strain as a function of load for the case of axial loading at an equilibrium condition and thermal control at 500 °F. The gage used for the plot is located on the skin side near the center of the panel and between the legs of a hat stiffener. The gage response is nearly linear below 17,000 lb, then bending is introduced and the gage response goes nonlinear. The bending strains are determined by the difference between the extrapolation of linear fit through the linear range and the indicated strain beyond the bending introduction point. The bending strains are then used in the single-gage F/S plot as shown in figure 12(b). This plot shows F/D as a function of the load, where D is the calculated bending strain of figure 12(a).

For these types of F/S plots, F/D values as low as 20 lb/μin./in. were not uncommon. The lower limit of the F/D values is arrived at as a result of experience gained from previous tests. The desire is to get the F/D value as low as possible without buckling the

panel, and therefore get a good prediction of the critical buckling load. To get a good approximation of the critical buckling load, a fitted range of the F/S curve needs to be selected. The fitted range is usually the lower portion of the F/S curve and is based on judgement and experience. In this case, the fitted range included the data for the last 2000 lb. For this case a straight line was drawn through the fitted range and the critical buckling is predicted to occur at 41,000 lb. Figure 12(b) does not provide the exact local buckling load (as explained in the Test Methods section) but this local prediction does provide an estimate of the general instability occurring in the panel. By averaging local buckling load predictions over an area of the panel away from the edges, a good estimate of the overall panel buckling load can be obtained. The single-gage method does, however, provide a good understanding of the local behavior of the panel (load path and mode changes can be readily observed) and is used to make real-time judgements of panel integrity.

For the buckling ΔT prediction case, the panel was loaded perpendicular to the hat stiffeners to a constant preload of 500 lb. The panel was then heated to equilibrium conditions at predetermined temperatures. A ΔT was maintained across the panel by keeping the edges parallel to the load at room temperature (fig. 11(d)). The panel was heated to 500 °F, stopping to record data at equilibrium temperatures of 200 and 250 °F. Figure 13(a) is a typical plot of strain as a function of temperature. The gage used for the plot is located on the skin side, near the center of the panel and between the legs of a hat stiffener. A linear fit was made through the first three data points and extrapolated out to the maximum test temperature. A bending curve was then projected starting at the third data point and ending at the last equilibrium data point. The square symbols on the projected bending curve represent possible equilibrium data point locations if an equilibrium condition had been reached at those temperatures.

The data points from the projected bending curve, including the one at the maximum temperature, were used in the $\Delta T/D$ plot shown in figure 13(b). This figure plots $\Delta T/D$ as a function ΔT, where D is the bending determined by the distance from the square symbols to the linear extrapolation line in figure 13(a). Performing a linear extrapolation through the last two data points of figure 13(b) to the ΔT axis provides a buckling ΔT prediction of approximately 560 °F. This prediction is sensitive to the selection of the projected bending curve of figure 13(a). Therefore the F/S curve may be steeper or shallower than the curve shown in figure 13(b), thus changing the prediction. To validate the projected bending curve, a test needs to be performed in which an equilibrium condition is reached at each of the square symbols of figure 13(a). This test was not performed because we did not realize the potential to predict a buckling ΔT until after this test configuration was completed. Therefore, the results are not conclusive but reveal only a potential approach to determining a buckling temperature.

For the transient temperature buckling load prediction cases, the panel was first loaded to a predetermined constant load. The skin side was then heated to 500 °F at a predetermined heating rate, thus introducing a through-the-thickness temperature gradient (fig. 11(f)). This process was repeated for multiple constant loads with each test providing a single data point. Figure 14(a) is a typical plot of strain as a function of load. The gage used for the plot is located on the skin side, near the center of the panel and between the legs of a hat stiffener. This plot shows that the panel was first loaded to 3000 lb, then the skin side was heated to 500 °F at a predetermined rate of 3.75 °F/sec. The gage then responded to the panel deformations caused by the temperature gradient (apparent strain has been accounted for in this plot). The gage output was monitored and the maximum attained bending strain was determined. After the maximum bending strains were determined for different constant load conditions, the single-gage F/S plot of figure 14(b) was obtained. Each point on the plot represents a different constant load condition. By fitting a straight line through the two higher load points, a buckling load of 4850 lb was obtained. By averaging multiple local buckling load predictions over an area of the panel, the overall panel buckling load can be obtained. As previously mentioned, it was not completely understood what type of support the edges parallel to the applied load had. Therefore the interpretation of the buckling prediction can not be properly understood. Also, more load points need to be considered to better define the curve of figure 14(b).

Table 1 shows selected comparisons between the analysis and test predictions of buckling load. The comparisons of the buckling temperatures for the ΔT across the panel case and the buckling load for the transient heating case were not included because of the

reasons previously mentioned. The pretest analysis predictions were derived from a NASTRAN finite element buckling analysis by McDonnell Douglas (Percy and Fields, 1990). The test predictions are based on an average of multiple measurements away from the edges of the panel. This provides a good estimate of the overall general instability of the panel. The averaging process involved 8 to 10 gages for each of the test configurations. The correlation was very good in all cases and the predictions were within 10 percent of the test indications.

CONCLUDING REMARKS

A single-strain-gage force/stiffness method has been developed and implemented as part of a test program to predict buckling loads and temperatures of a hat-stiffened panel. The method was developed as a result of a need to predict buckling without using back-to-back strain gages. The panel was heated and loaded in a variety of configurations and test predictions were made and compared with analytical predictions. The test predictions correlated well with the analytical solutions. The correlations support the validity of the single-gage force/stiffness method applied to this test. The method also proved to be a useful real-time prediction technique for determining the panel integrity. More investigation into this method needs to be done to better define the guidelines for the use of the single-gage force/stiffness method.

ACKNOWLEDGMENTS

The authors would like to acknowledge Roger Fields of Ames-Dryden for his extensive contributions to the development of this single-strain-gage F/S method. The authors would also like to acknowledge the McDonnell Douglas Corporation for providing the test panel and support on this project.

REFERENCES

Greene, Bruce E., *Substantiation Data for Advanced Beaded and Tubular Structural Panels. Volume 1, Design and Analysis*, NASA CR-132460, 1974.

Jones, Robert E., and Greene, B.E., "The Force/ Stiffness Technique for Nondestructive Buckling Testing," AIAA paper no. 74-351, April 1974.

Ko, William L., Shideler, John L., and Fields, Roger A., *Buckling Characteristics of Hypersonic Aircraft Wing Tubular Panels*, NASA TM-87756, 1986.

Percy, Wendy C., and Fields, Roger A., "Buckling of Hot Structures," *Eighth National Aero-Space Plane Symposium* paper no. 38, March 1990.

Zamanzadeh, B., Trover, W.F., and Anderson, K.F., "DACS II - A Distributed Thermal/Mechanical Loads Data Acquisition and Control System," International Telemetering Conference Paper, July 1987.

Table 1. Comparison of buckling loads (Percy and Fields, 1990).

Prediction	Cross corrugation load, lb			Axial load, lb	
	Room temperature	Panel to frame temperature gradient	500 °F	Room temperature	500 °F
NASTRAN	−6,500	−4,200	−5,500	−39,700	−36,900
Test	−6,400	−4,400	−5,600	−41,700	−39,200

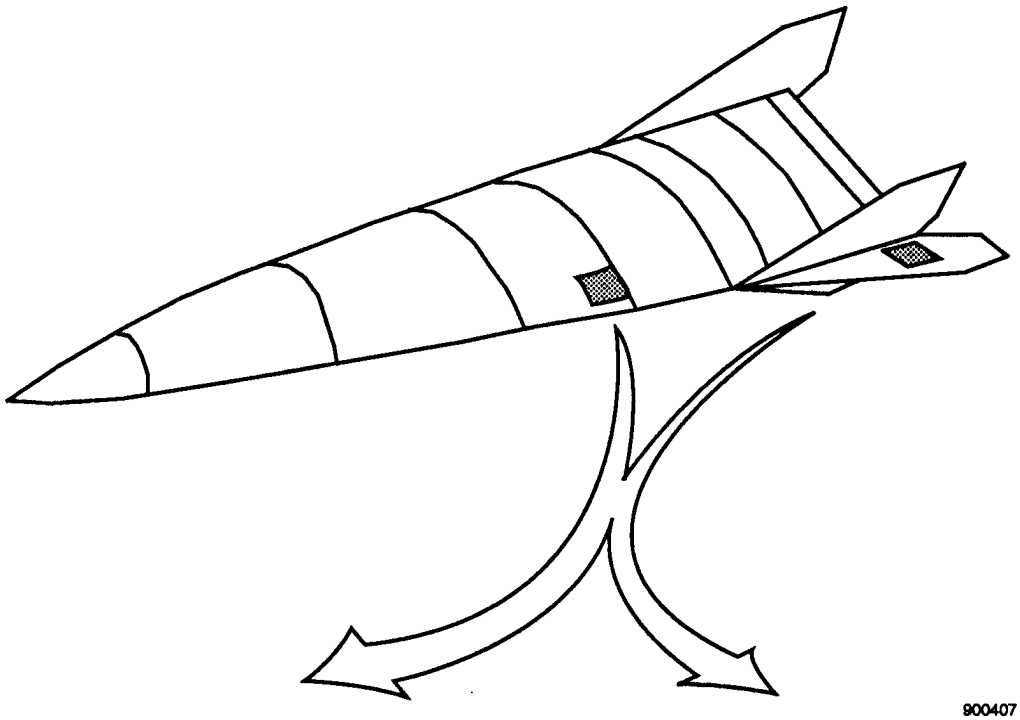

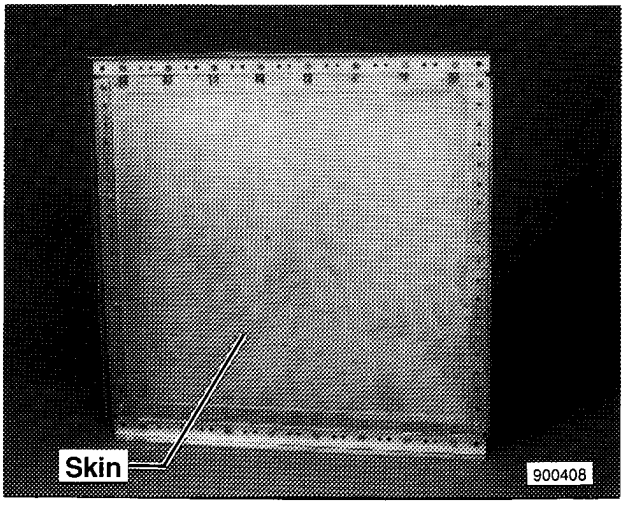

(a) Skin side.

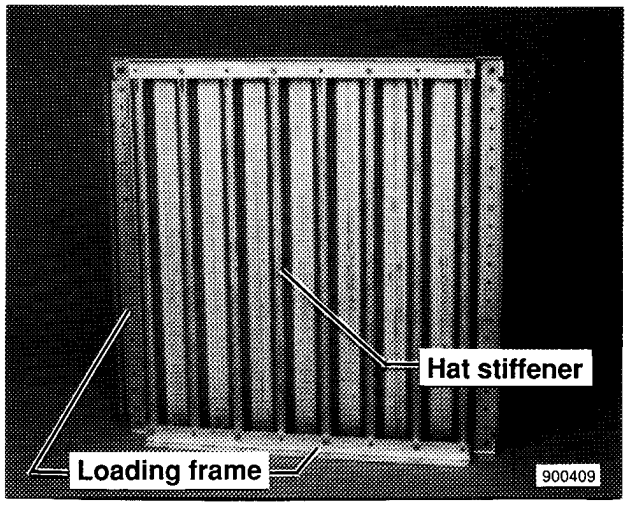

(b) Hat side.

Figure 1. Monolithic Ti 6A1-4V hat-stiffened panel.

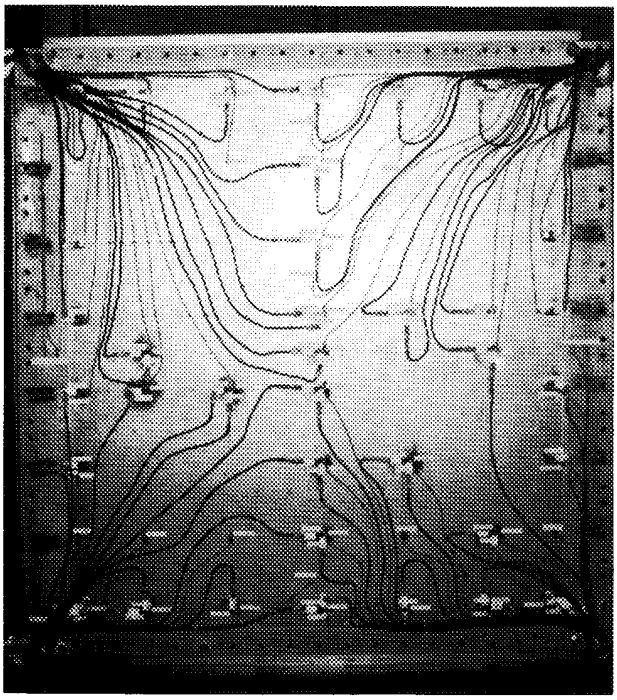

EC89 53-18

(a) Skin side.

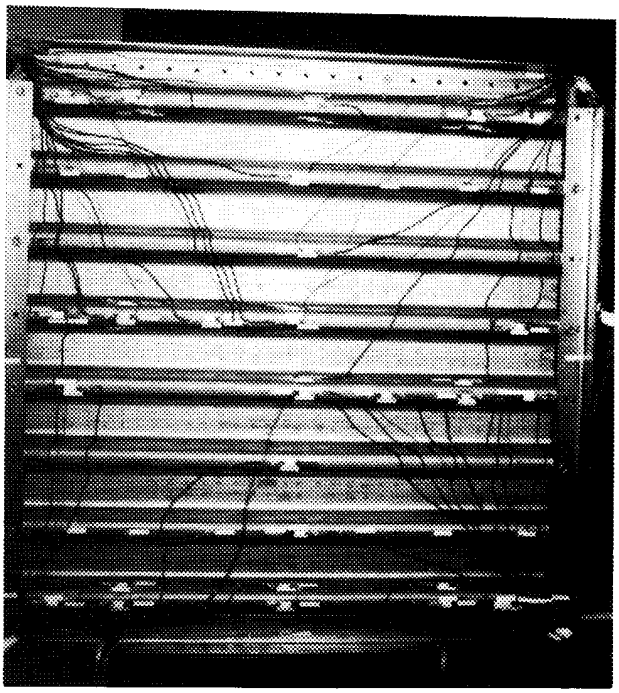

EC89 53-23

(b) Hat side.

Figure 2. Hat-stiffened panel intrumentation.

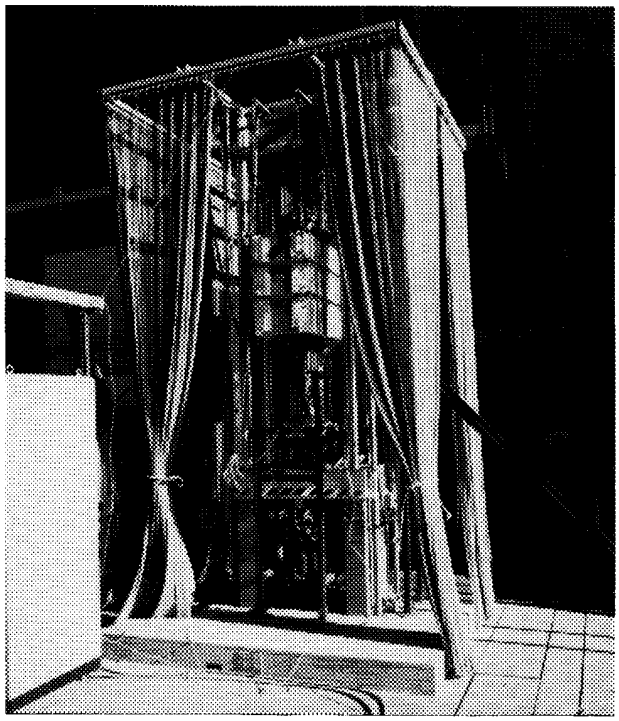

EC89 38-1

Figure 3. The 220-kip load frame system.

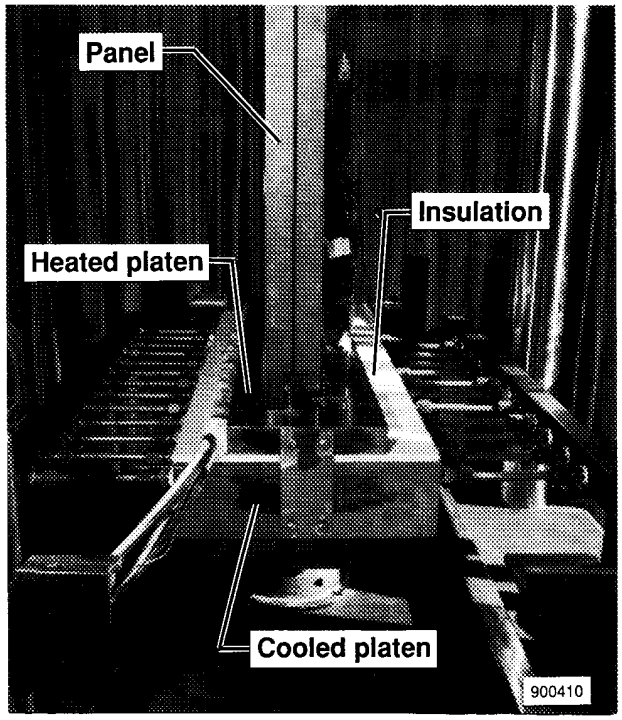

Figure 4. Load platen design.

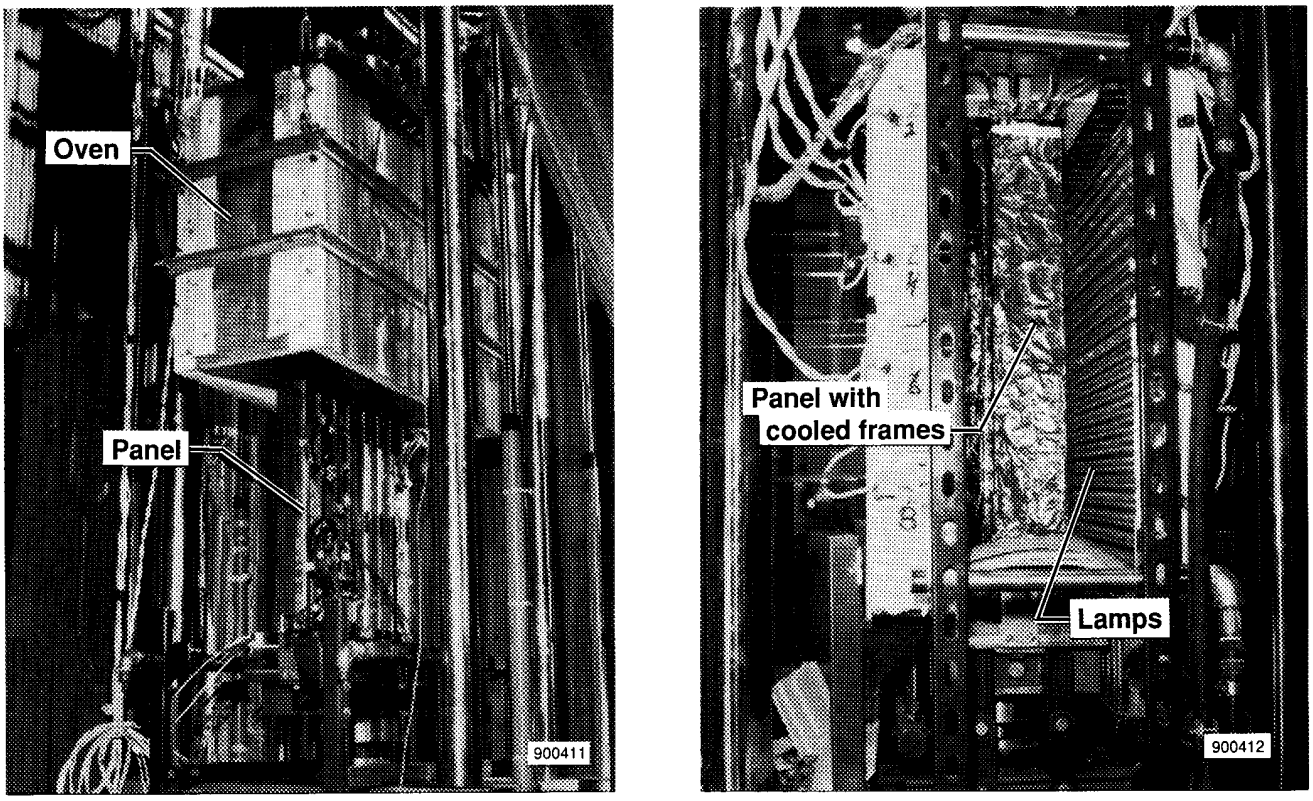

(a) Outer view of oven with buckling panel.

(b) Inner view of oven with buckling panel.

Figure 5. Oven design

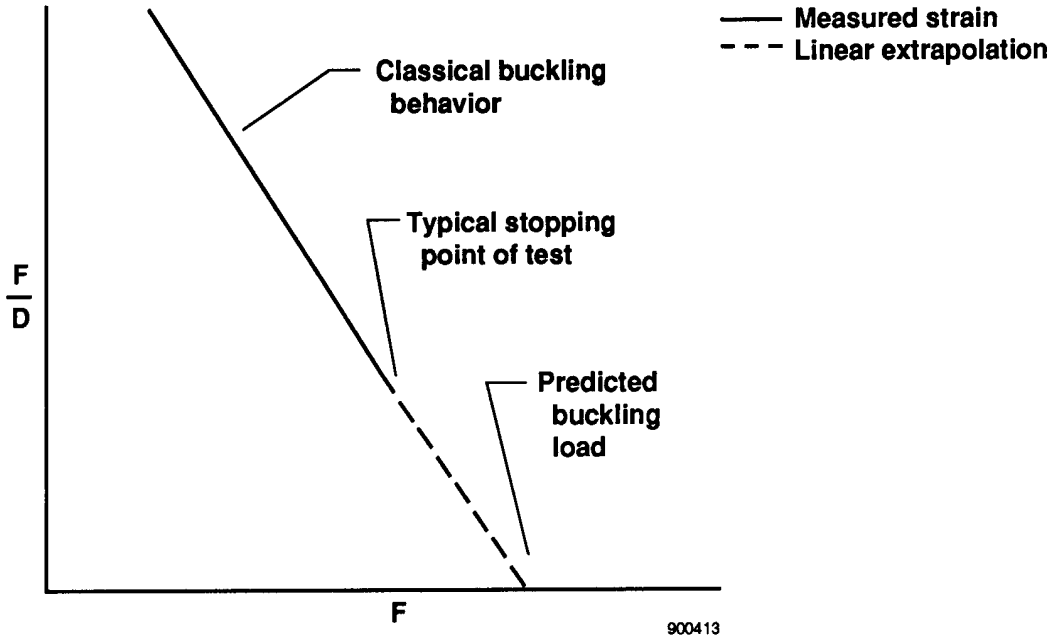

Figure 6. Classical force/stiffness plot for the case of general instability.

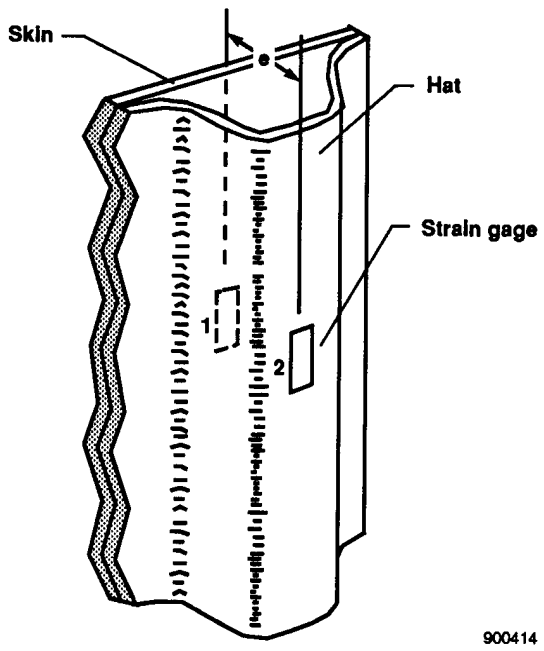

(a) Eccentric gages.

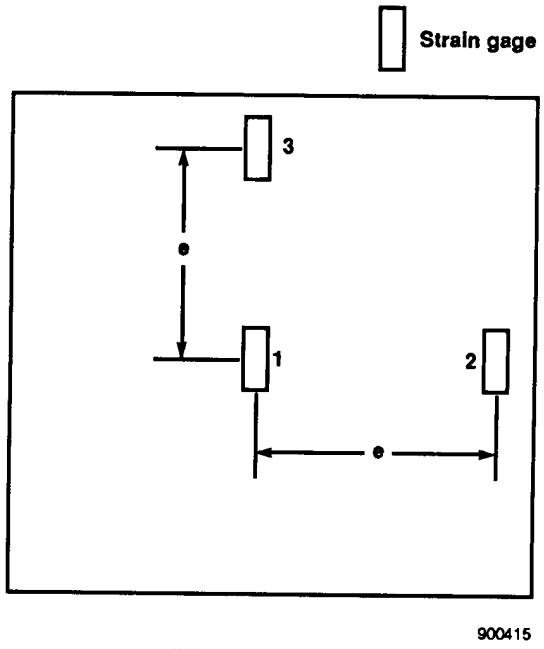

(b) Offset gages.

Figure 7. Available instrumentation layouts for two gage force/stiffness method.

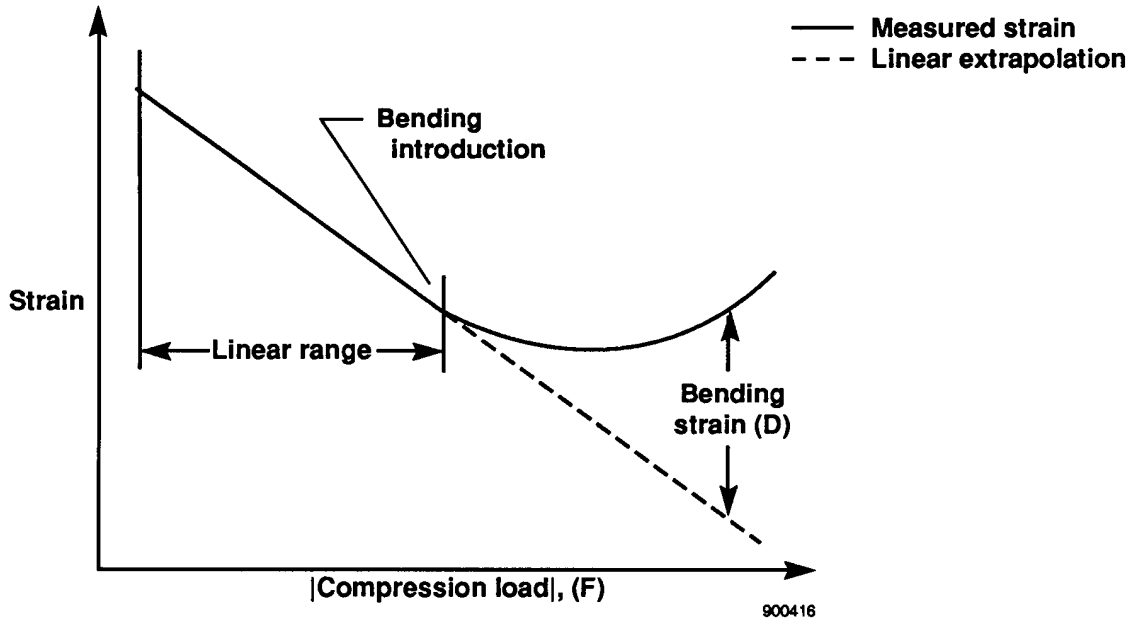

(a) Typical strain output as a function of load.

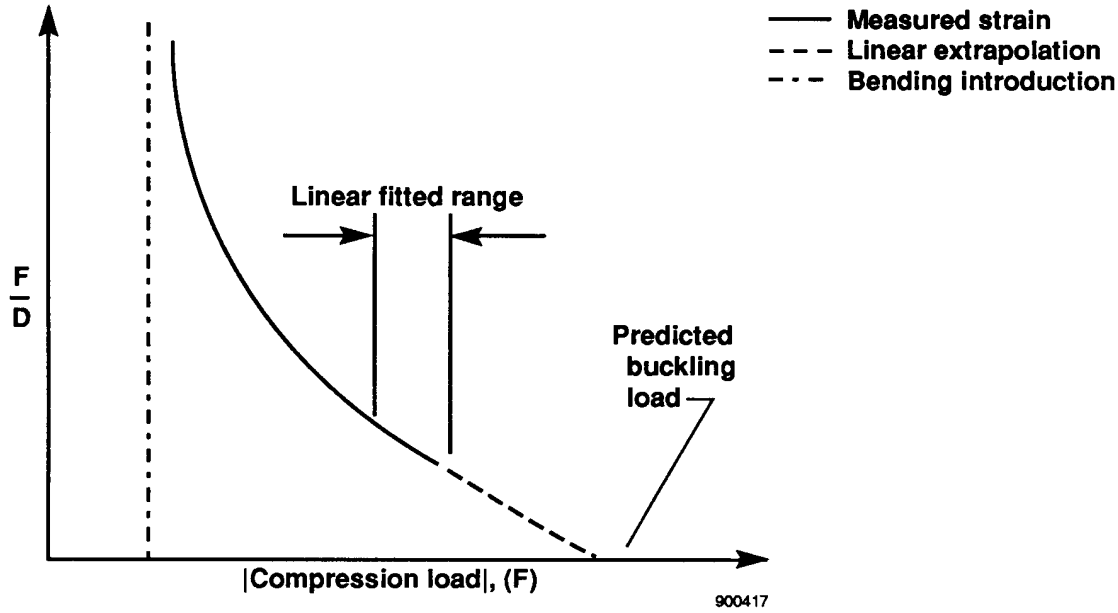

(b) Typical force/stiffness plot.

Figure 8. Single-gage force/stiffness method of predicting the buckling load under isothermal heating.

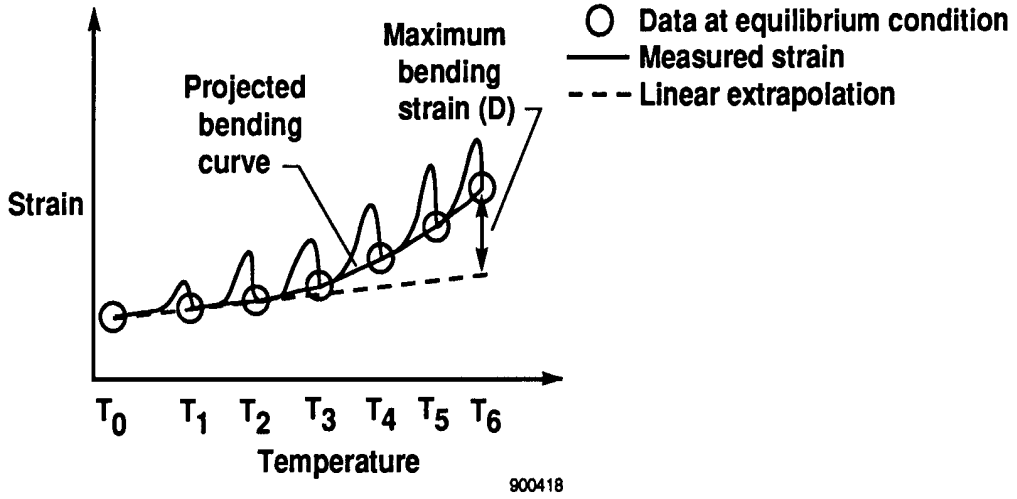

(a) Expected strain output as a function of temperature.

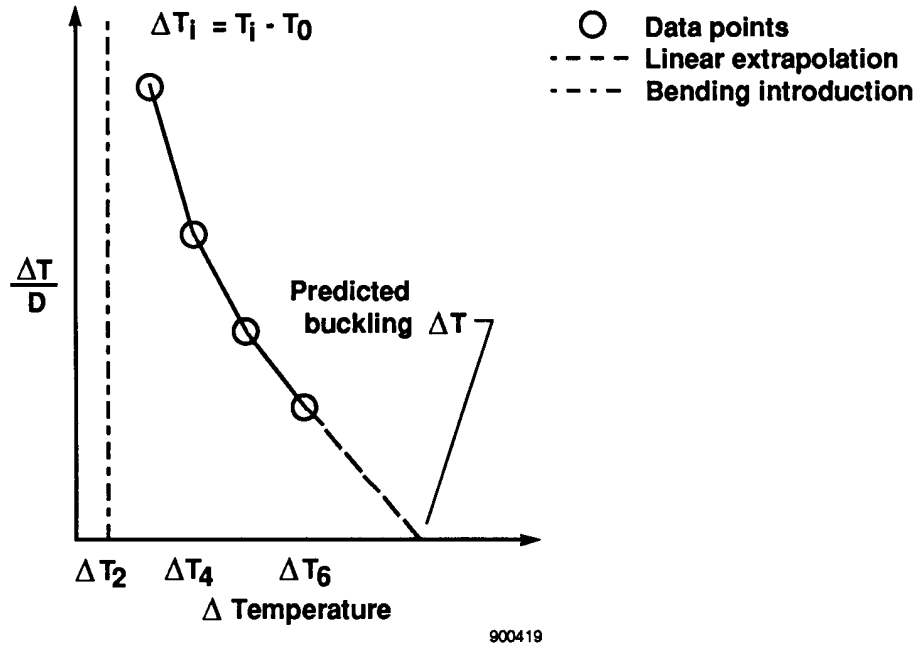

(b) Typical temperature/stiffness plot

Figure 9. Single-gage temperature/stiffness method for predicting the buckling Δ temperature under isothermal heating with a known ΔT.

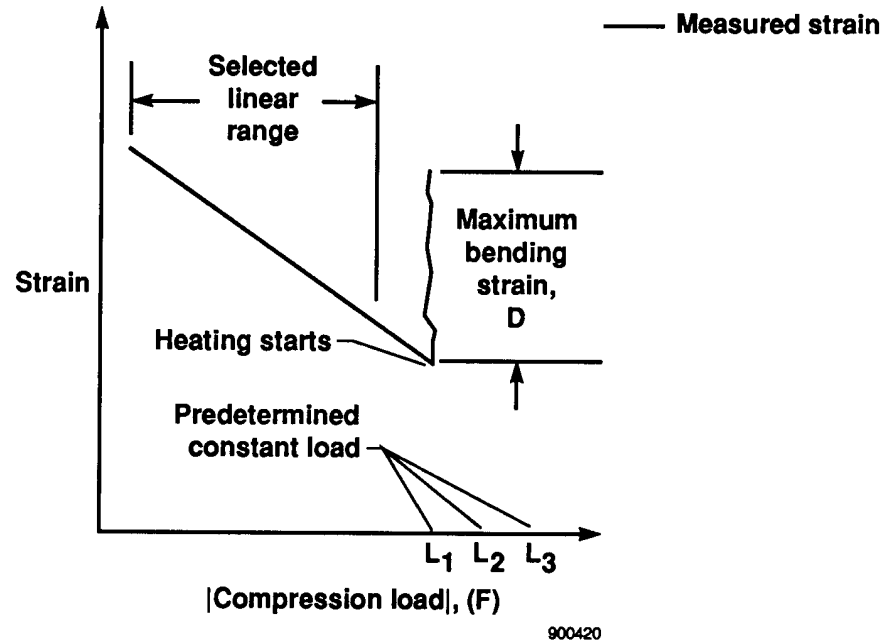

(a) Typical strain output as a function of load.

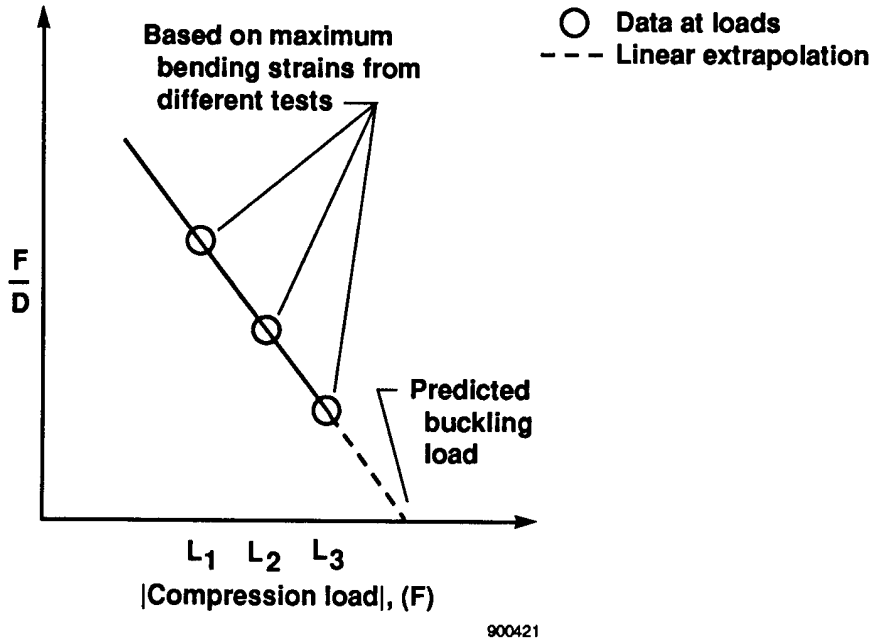

(b) Typical force/stiffness plot.

Figure 10. Single-gage force/stiffness method of predicting the buckling load under transient heating at a constant load.

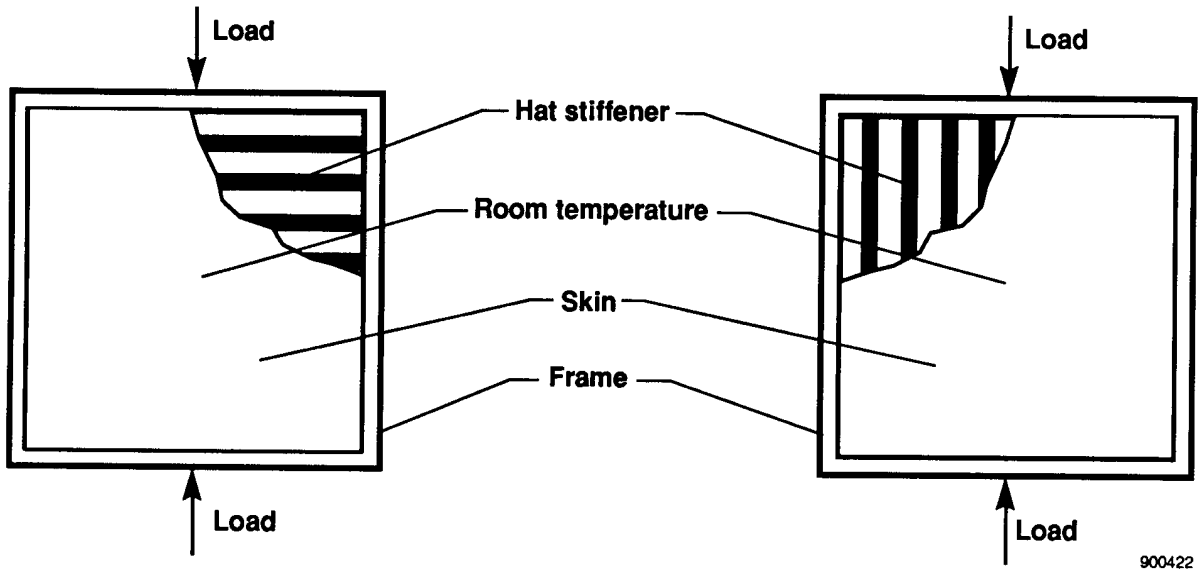

(a) Panel at room temperature with load applied perpendicular to hat stiffeners.

(b) Panel at room temperature with load applied parallel to hat stiffeners.

Figure 11. Test configurations.

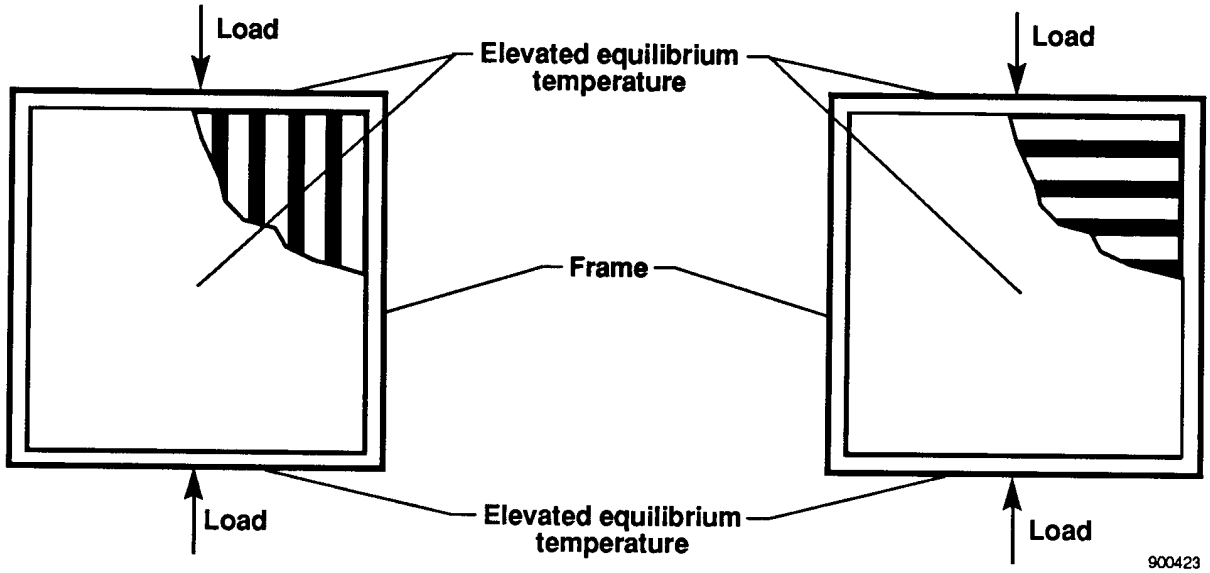

(c) Panel at an elevated temperature with load applied parallel to hat stiffeners

(d) Panel at an elevated equilibrium temperature with load applied perpendicular to hat stiffeners.

Figure 11. Continued.

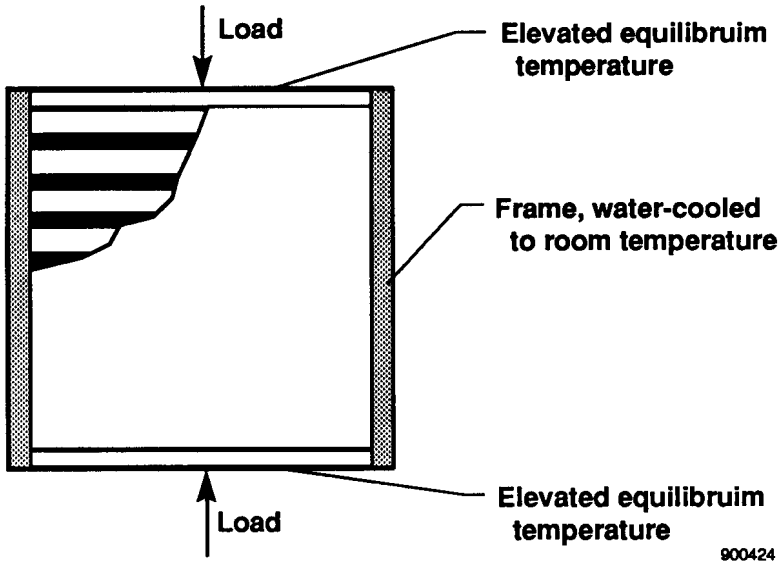

(e) Across-the-panel temperature gradient with load applied perpendicular to hat stiffeners.

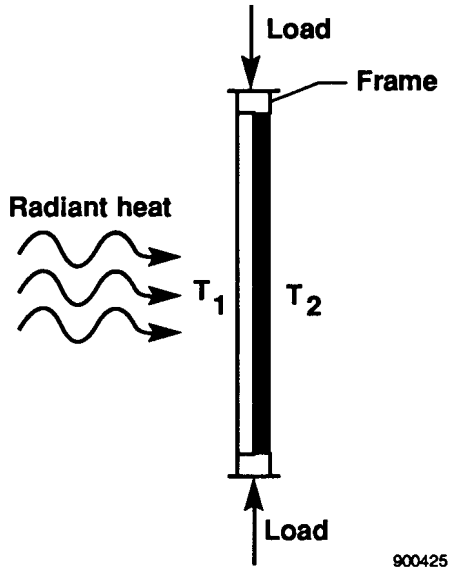

(f) Through-the-thickness temperature gradient with load applied parallel to hat stiffeners.

Figure 11. Concluded.

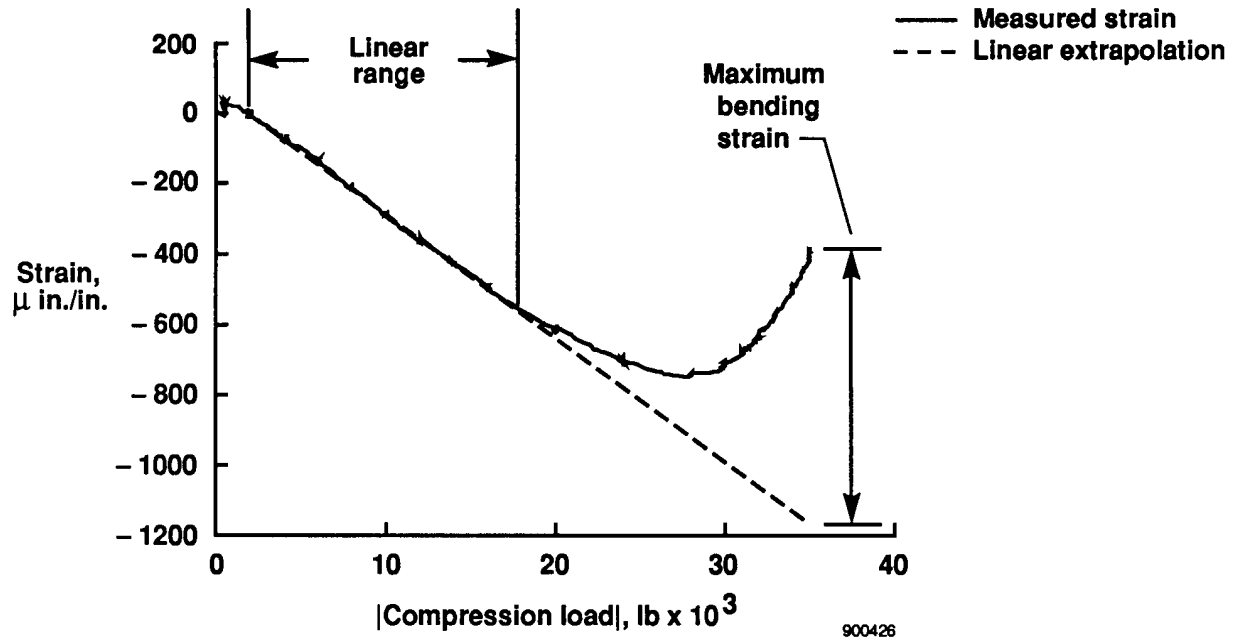

(a) Typical strain output as a function of load.

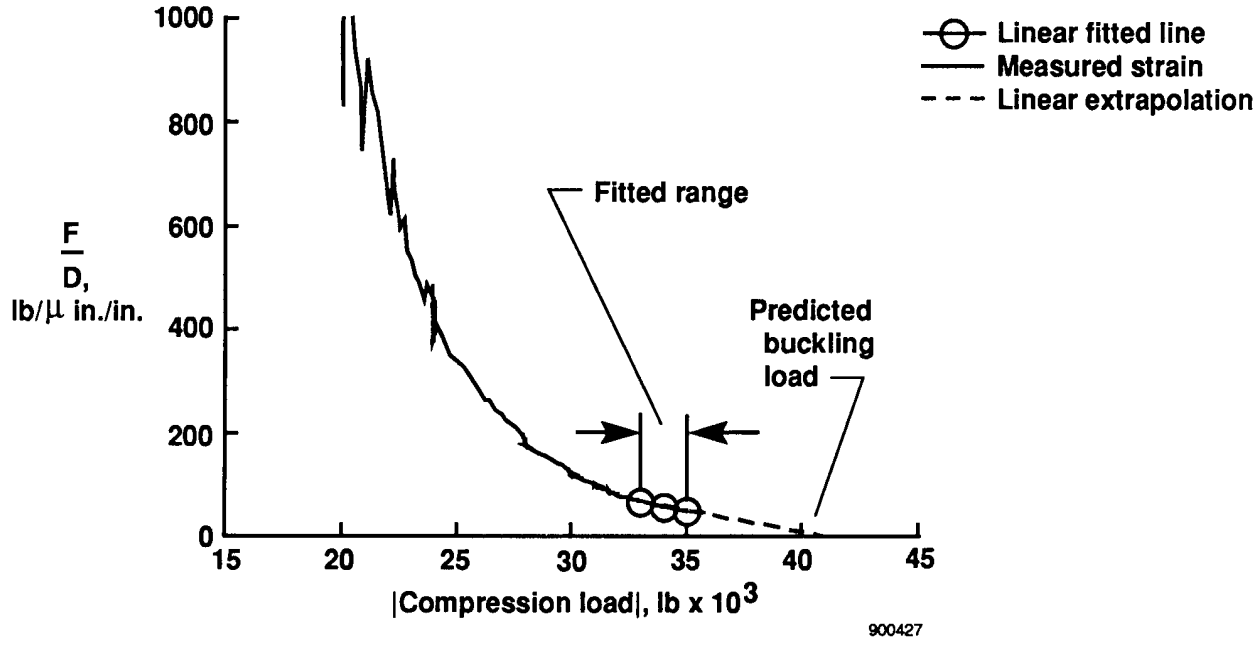

(b) Typical force/stiffness plot.

Figure 12. Typical prediction of buckling load at an elevated temperature equilibrium condition and thermal control at 500 °F.

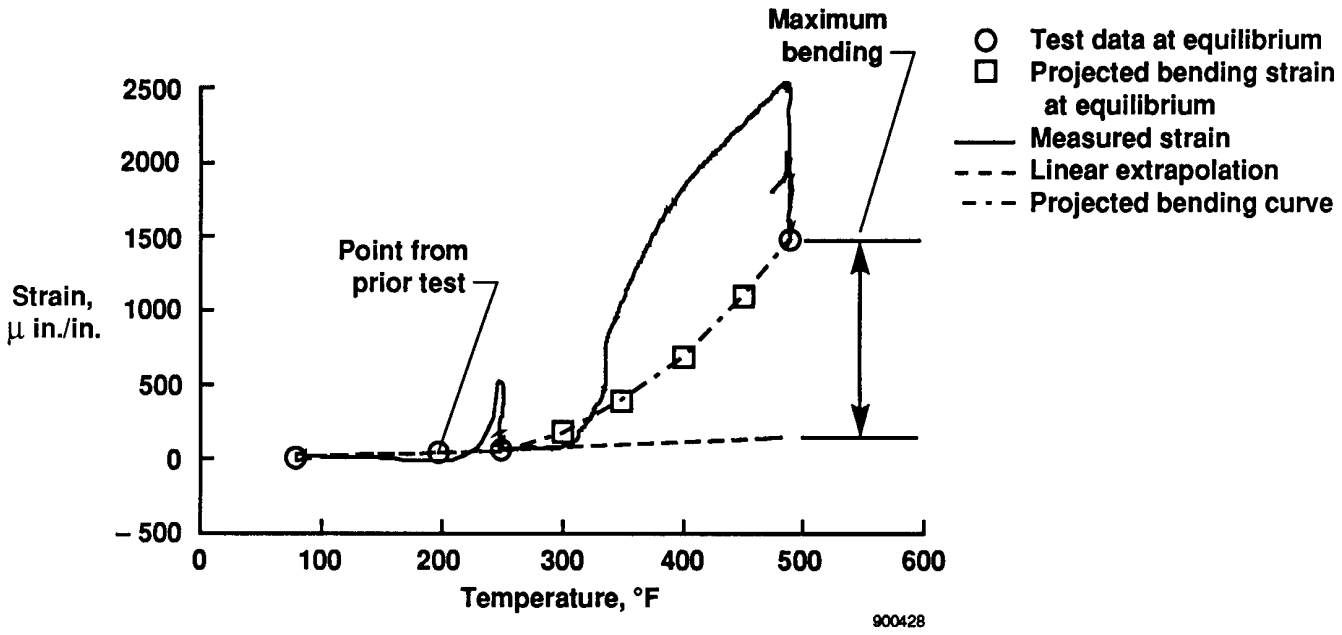

(a) Typical strain as a function of temperature.

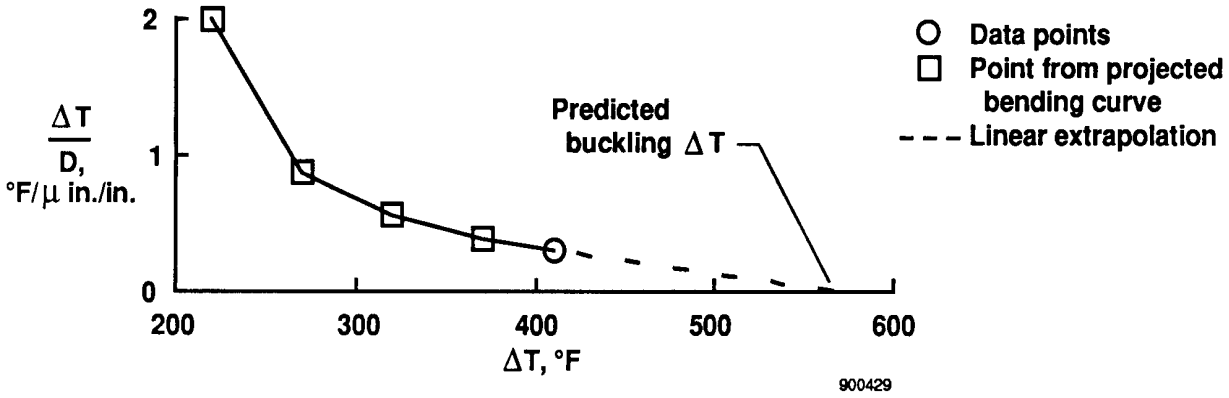

(b) Typical $\Delta T/D$ plot, where ΔT is the difference between the hot-panel and cooled-frame temperatures.

Figure 13. Typical buckling ΔT prediction for a strain gage located near the center of the panel and in the middle of a hat stiffener.

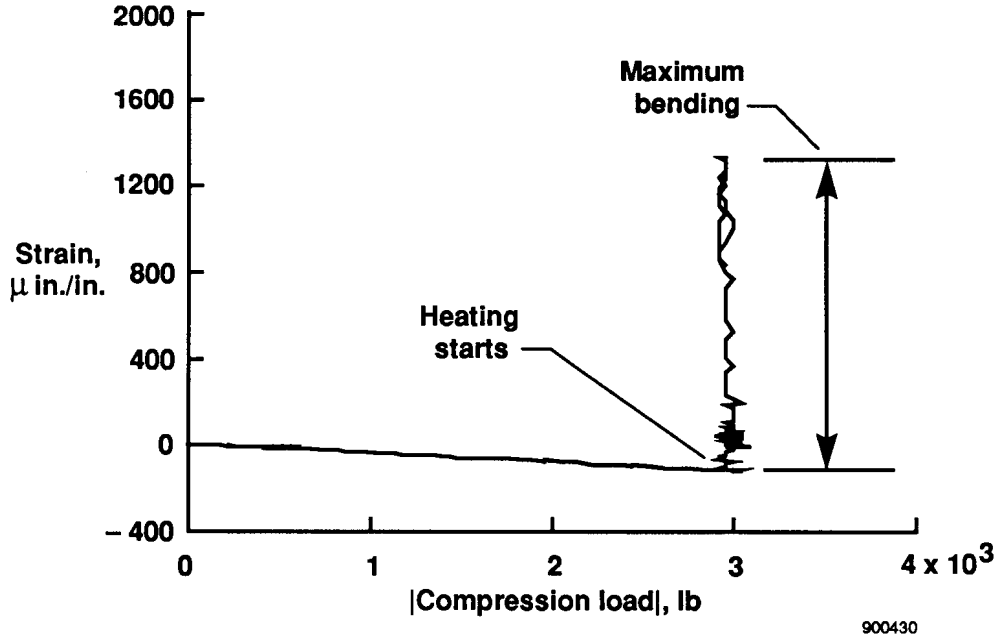

(a) Typical strain output as a function of load.

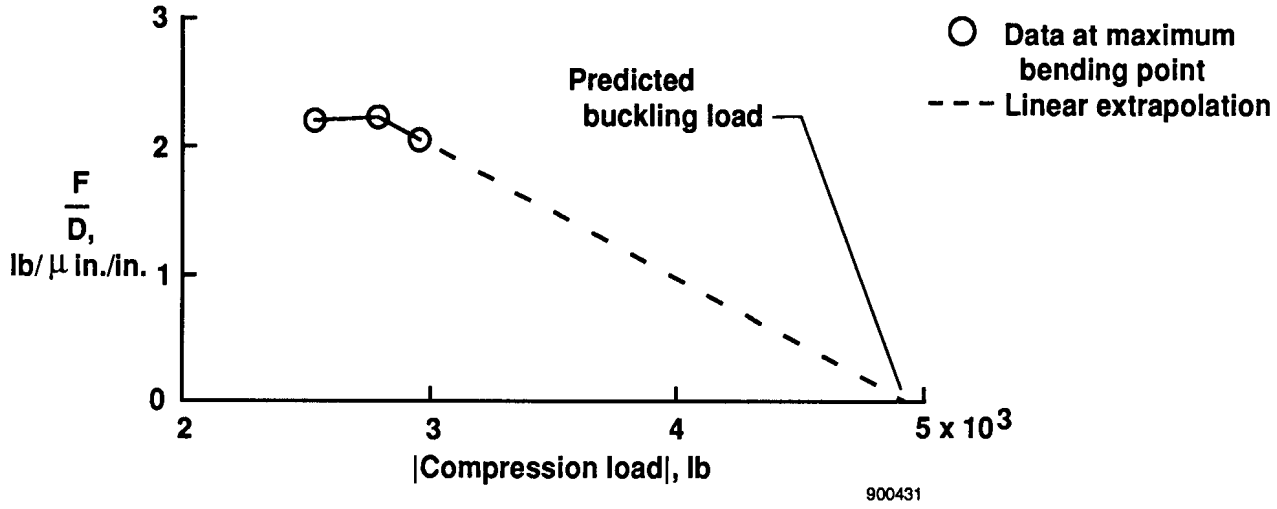

(b) Typical force/stiffness plot.

Figure 14. Typical prediction of the buckling load under transient heating at a constant load.

NASA
National Aeronautics and Space Administration

Report Documentation Page

1. Report No.	2. Government Accession No.	3. Recipient's Catalog No.
NASA TM-101733		

4. Title and Subtitle

Single-Strain-Gage Force/Stiffness Buckling Prediction Techniques On A Hat-Stiffened Panel

5. Report Date

February 1991

6. Performing Organization Code

7. Author(s)

Larry D. Hudson (Ames Research Center, Dryden Flight Research Facility, Edwards, California)
Randolph C. Thompson (PRC Systems Services, Edwards, California)

8. Performing Organization Report No.

H-1660

10. Work Unit No.

RTOP 505-63-31

9. Performing Organization Name and Address

NASA Ames Research Center
Dryden Flight Research Facility
P.O. Box 273, Edwards, California 93523-0273

11. Contract or Grant No.

13. Type of Report and Period Covered

Technical Memorandum

12. Sponsoring Agency Name and Address

National Aeronautics and Space Administration
Washington, DC 20546-3191

14. Sponsoring Agency Code

15. Supplementary Notes

Presented at the ASME Structures and Materials Conference, Dallas, Texas, November 25–30, 1990.

16. Abstract

Predicting the buckling characteristics of a test panel is necessary to ensure panel integrity during a test program. A single-strain-gage buckling prediction method was developed on a hat-stiffened, monolithic titanium buckling panel. The method is an adaptation of the original force/stiffness method which requires back-to-back gages. The single-gage method was developed because the test panel did not have back-to-back gages. The method was used to predict buckling loads and temperatures under various heating and loading conditions. The results correlated well with a finite element buckling analysis. The single-gage force/stiffness method was a valid real-time and post-test buckling prediction technique.

17. Key Words (Suggested by Author(s))	18. Distribution Statement
Elevated temperatures; foil strain gages; force/stiffness; hat-stiffened panel; hypersonic vehicle; NASTRAN; overall panel buckling	Unclassified-Unlimited Subject category 05

19. Security Classif. (of this report)	20. Security Classif. (of this page)	21. No. of Pages	22. Price
Unclassified	Unclassified	22	A02

For sale by the National Technical Information Service, Springfield, Virginia 22161-2171